IEEE Access
Multidisciplinary | Rapid Review | Open Access Journal

Received November 12, 2018, accepted December 19, 2018, date of publication December 24, 2018,
date of current version January 16, 2019.

Digital Object Identifier 10.1109/ACCESS.2018.2889461

Proximity Effects of Lateral Conductivity Variations on Geomagnetically Induced Electric Fields

CHUNMING LIU[1], XUAN WANG[1], CHENXIANG LIN[2], AND JINGYU SONG[3]
[1]School of Electrical and Electronic Engineering, North China Electric Power University, Beijing 102206, China
[2]Electric Power Research Institute, State Grid of Fujian, Fujian 350000, China
[3]China State Shipbuilding Corporation System Engineering Research Institute, Beijing 100036, China

Corresponding authors: Chunming Liu (cm_liu@163.com) and Xuan Wang (x_wang@ncepu.edu.cn)

This work was supported in part by the National Key Research and Development Plan under Grant 2016YFC0800103, in part by the National Natural Science Foundation of China under Grant 51677068, and in part by the Fundamental Research Funds for the Central Universities under Grant 2018QN007.

ABSTRACT During a magnetic storm, the induced geoelectric field drives geomagnetically induced currents (GIC) in power transmission networks, railway systems, and pipelines, negatively affecting these systems. In regions with complex geological structures, the lateral earth conductivity changes influence the induced electric field distribution in the earth. H- and E-polarization are two cases of the orientation of the E-field vector relative to the lateral changes. A model of the earth with lateral conductivity changes is established in this paper to examine the effects of conductivity change across a discontinuity on the magnitude of the E-field for the case of the E-field parallel to the discontinuity. The electric field distribution with distance from the discontinuity is calculated, and the relationship between the lateral conductivity changes and electric field distortion is analyzed using the finite element method. In addition, the GIC variation in the power grid due to the lateral conductivity changes is examined. Then, the factors affecting GIC, including conductivity, frequency, and distance, are investigated. The results show that lateral conductivity changes can influence the GIC in power lines running parallel to the discontinuity up to 250 km from the discontinuity. The methods and results are significant for understanding how lateral conductivity changes influence GIC and will improve the accuracy of GIC calculations.

INDEX TERMS Finite element method (FEM), geomagnetically induced currents (GIC), proximity effect.

I. INTRODUCTION

Geoelectric fields are induced by variations in the magnetic field of the Earth during magnetic storms and drive geomagnetically induced currents (GIC) in railways, pipelines, and electric power systems. In a power grid, GIC flow in the circuit consisting of transmission lines, grounded neutral conductors of transformers, and the Earth [1]. The GIC in a power grid can be considered as quasi-DC currents and cause bias fluxes and half-cycle saturation in transformers [2].

In the modeling of GIC in a power grid [3], the effects of geomagnetically induced electric fields on the power grid are taken to be equivalent to a set of voltage sources imposed on its transmission lines between various grounded points. The value of the voltage source depends on the integral of the geoelectric field along the line between grounded neutral conductors of the transformers. If the geoelectric field distribution is well known, the GIC calculations can be converted into a circuit problem [4]. Therefore, to assess the influence of lateral conductivity changes on GIC, the effects of lateral changes in the Earth conductivity on the geoelectric field should first be evaluated [5].

In the previous work, a line current was used to simulate an electrojet. The integral expressions for the electromagnetic fields at the surface of a layered earth were numerically integrated for two simple models, one representing an average continent, and the other representing an active tectonic area [6]. The two-dimensional (2-D) conductivity model has been previously used by Weaver in 1963. A numerical method was also developed to solve the appropriate differential equations and conditions. The two polarization cases were solved, and the fields and current distributions were determined [7] [8]. The field distributions and surface effects

of the 2-D conductivity inhomogeneities were investigated based on the above. The inhomogeneities of different thicknesses at the Earth's surface and those of fixed sizes, but at various depths, were considered [9]. However, geophysicists have performed research with the objective of obtaining the conductivity distribution underground [10]. In addition to the amplitude of the geomagnetic disturbances (GMD), the frequency of the magnetic field variations and geoelectrical structures can also be used to determine the electric field distribution. The recorded GIC data show that the Earth conductivity significantly impacts the GIC in power systems [11]. The uneven distribution of the induced currents resulting from conductivity variation is the main factor impacting geoelectric field distortion compared to the E-field in a uniform Earth [4]. Moreover, the effects of lateral Earth conductivity variation on geoelectric fields and GIC have not yet been characterized as a function of both distance from the interface of regions with different conductivity and depth below the surface.

The effects of lateral variation of the Earth conductivity structures on geoelectric fields depend on the E- and H-polarization and on the orientation of the electric field vector relative to the direction of the discontinuity [7]. The variation of the intensity of the E-field with distance from a discontinuity in conductivity can also be called a proximity effect [12]. The term "proximity effect" commonly refers to electromagnetic compatibility between nontouching conductors; however, the proximity effect in geoelectric fields involves the interaction between touching conductors on the Earth. This effect influences the electric field parallel to the lateral discontinuity in the conductivity. Due to the differences in the Earth conductivity, there are discrepancies between the geoelectric fields and telluric currents induced at two sides of the interface of different conductivity. The telluric currents change the geoelectric field distribution in the adjacent area, which is particularly evident at the interface of different conductivity. As the component of the electric field which is tangential to the discontinuity in conductivity is continuous, the proximity effect makes the electric field intensity near the discontinuity change gradually with distance from the discontinuity. If the transmission line is parallel to the interface, the proximity effect may significantly impact the GIC in power grids. The geoelectric field model used in the finite element modelling of the effect of the discontinuity is illustrated in Fig. 1.

To assess the variation of the intensity of an E-field parallel to discontinuity in Earth conductivity, we develope a 2-D Earth conductivity model to predict the geoelectric field distribution and GIC. The numerical results demonstrate the correlations among the conductivity variations, GMD frequency, and geoelectric field distortion. We then evaluate the influences of the geographical distribution of the electric field on the GIC in power grids. The influence of lateral discontinuities in conductivity on geoelectric fields should be considered comprehensively.

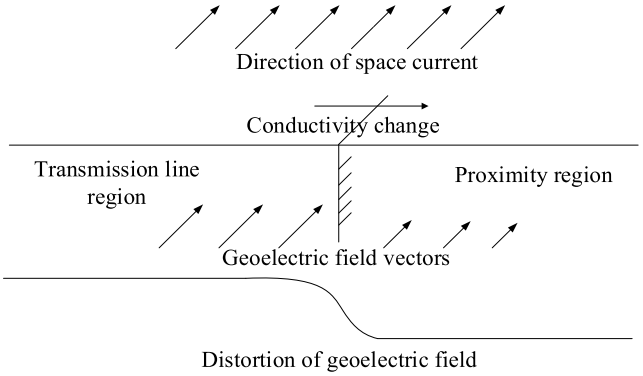

FIGURE 1. Model to illustrate the proximity effect on the tangential E-field.

II. MODEL AND METHODS

A. GEOELECTRIC FIELD MODEL

While geomagnetic field variations occur on a global scale, the span of a regional power grid is usually less than 1000 km, even in the case of long-distance ultra-high-voltage transmission. Therefore, it is not necessary to adopt a global model of the Earth conductivity structures, so we instead model the Earth as an infinite half-space, with a planar air-Earth interface, neglecting its curvature [14]. A small portion of the entire Earth conductor is considered to reduce the size of the model to a scale that can be easily represented by a finite element model. To simplify the calculations, the solution domain is taken as a rectangular block. A three-dimensional (3-D) block model with lateral conductivity variations is established to study the specific effects of the conductivity variations on one side of the discontinuity on the E-field intensity in the adjacent area, as shown in Fig. 2.

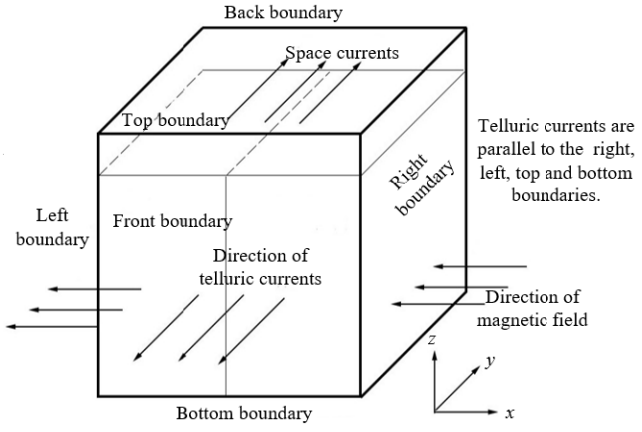

FIGURE 2. 3-D geoelectric field model of E-field in a conduction medium.

In the Cartesian coordinate system, x points in the direction of the conductivity changes, y points in the direction of the horizontal extension of the discontinuity, and z points upwards. The Earth conductivity model consists of two regions with constant conductivities. The interface of

the sudden change is set at $x = 0$, which could represent a coastline, plate boundary, or rock fracture surface. The transmission line is located in the region with $x < 0$, and the area with $x > 0$ is called the ''proximity region.'' The space currents are assumed to span both the ''transmission line region'' and the ''proximity region''.

Since GMD have frequencies of 0.0001–0.1 Hz and GIC thus can be considered to be quasi-DC, we perform the simulations in the telluric current field [15]. The conduction current of the Earth is significantly greater than the displacement current. Therefore, we consider only the conduction current density in the electromagnetic calculations. We make the following assumptions: the electric field is produced only by the magnetic field variations, irrespective of the electric field produced by stationary charges in the Earth, which can be easily understood based on Faraday's law [5], [16]; all of the magnetic permeability values in the solution domain are equal to the vacuum permeability, $\mu_0 = 4\pi \times 10^{-7}$H/m; the Earth conductor is isotropic and the conductivity does not change with time; the conductivity of each structure do not vary spatially; and abrupt conductivity variation occur only at the interface between the two regions.

B. CURRENT SOURCE MODEL

When a geomagnetic storm occurs, the geomagnetic field variations obtained using geomagnetic observatories are mainly caused by the ionospheric currents deriving from localized substorms on the nightside during disturbed times. It is known that the altitude of the ionospheric currents varies between 100 and 300 km [16]. We can suppose they are located 100 km above the surface of the Earth as reference [17] did. The shape of the spatially equivalent current model can affect the induced geoelectric field distribution. In this study, the space currents are represented by a surface current sheet with infinite extent in the y-direction and a lateral width of 1600 km, being identical to that of the model. The magnetic field produced by a surface current sheet which is infinite in both the x-and y-directions is a uniform planar magnetic field. In the model presented here, the infinite current sheet is approximated by a current sheet with a lateral extent equal to that of the modelled region. The edge effects beyond the edge of the current sheet are thus neglected. With this model for the space currents we mainly focus on the influence of the regional conductivity differences on the lateral variation of the E-field near the discontinuity between the regions of the Earth with different conductivities.

The space current density is set to 1 A/m, changing sinusoidally over time. The current source is located at a height above the surface of the Earth z of 100 km. The sinusoidally varying surface currents could drive the geoelectric field with the same waveform, although actual geomagnetic fields change with nonsinusoidal forms, which can be regarded as the superposition of multiple sinusoidal sources. The frequency of the surface currents is set in the range of that of the geomagnetic field variations. It is possible not only to research how the GMD frequency f affects the geoelectric field distortions, but also to explore the influence of lateral conductivity variations on GIC with varying frequencies in power grids.

Generally, the magnetic field produced by space currents can be calculated directly using Ampere's law. Then, the wave impedance formula is adopted to analyze the geoelectric field intensity. However, this method does not account for the skin and eddy current effects; that is, the electric field is generated only by the primary field. Therefore, the problem should be attributed to an eddy current field. In this study, we consider the time-harmonic electromagnetic field and the calculated field quantities are amplitudes rather than RMS (Root Mean Square) values, such as the maximum surface electric field, voltage, and GIC.

C. BOUNDARY PROBLEM SIMPLIFICATION

A 3-D eddy current field can be expressed mathematically using the magnetic vector and scalar potentials. The governing equations are

$$\nabla \times \frac{1}{\mu} \nabla \times \boldsymbol{A} + \gamma \left(\frac{\partial \boldsymbol{A}}{\partial t} + \nabla \varphi \right) = \boldsymbol{J}_S \tag{1}$$

And

$$\nabla \cdot \gamma \left(\frac{\partial \boldsymbol{A}}{\partial t} + \nabla \varphi \right) = 0, \tag{2}$$

where $\boldsymbol{J}_S$ is the density of the current source. There is no current source in the Earth conductor, so $\boldsymbol{J}_S = \boldsymbol{0}$. $\boldsymbol{A}$ and φ respectively express vector potential and scalar potential, γ is the conductivity of Earth. The permeabilities of air and the Earth are both assumed to be μ_0.

The space currents are set as the upper boundary of the model. The surface current density $\boldsymbol{K}$ is applied, and the tangential component of the intensity of the magnetic field acting on it is obtained from a geomagnetic observatory. The boundary conditions can be expressed by the magnetic vector potential in (3):

$$\boldsymbol{e}_z \times (\frac{1}{\mu_0} \nabla \times \boldsymbol{A}) = \boldsymbol{K}, \tag{3}$$

where e_z is the normal unit vector of the upper boundary, which points in the positive z-direction. In an actual situation, if observational geomagnetic data have been obtained, they can be converted into the surface current density components K_x and K_y. In this case, the ground is set as the upper boundary. It is possible to determine subsequently how the geoelectric field varies using observational magnetic data.

The boundary conditions on the left and right are set based on the space current model. For E-fields with orientation parallel to the conductivity interface, the space currents point in the y-direction. The telluric currents induced by equivalent space currents flow along the y-direction into the front and back boundary surfaces. Thus, the boundary condition is given by

$$A_1 = A_2. \tag{4}$$

where the subscripts 1 and 2 refer to the transmission line region and the proximity region respectively. The telluric currents are parallel to the left and right boundary surfaces. Accordingly,

$$\boldsymbol{e}_x \times \left(\frac{1}{\mu_0}\nabla \times \boldsymbol{A}\right) = 0. \tag{5}$$

At the interface, the electromagnetic field distribution is so complicated that it is difficult to determine the boundary conditions [18]. Therefore, to facilitate the application of boundary conditions, the interface is set midway between the left and right boundary surfaces of the model. The boundary conditions above can be written as

$$e_x \times \frac{1}{\mu_0}\left(\nabla \times \boldsymbol{A}_1 - \nabla \times \boldsymbol{A}_2\right) = 0, \tag{6}$$

$$\boldsymbol{A}_1 = \boldsymbol{A}_2, \tag{7}$$

$$\varphi_1 = \varphi_2, \tag{8}$$

and

$$\boldsymbol{e}_x \cdot \gamma_1 \left(j\omega \boldsymbol{A}_1 + \nabla\varphi_1\right) = \boldsymbol{e}_x \cdot \gamma_2 \left(j\omega \boldsymbol{A}_2 + \nabla\varphi_2\right), \tag{9}$$

where $\boldsymbol{A}_1$ and $\boldsymbol{A}_2$ are the magnetic vector potentials on the two sides of the interface, φ_i is the electric scalar potential, and γ_i is the conductivity ($i = 1, 2$).

The lower boundary of the modelled region should extend well beyond the skin depth of the electromagnetic field. Although the frequencies of GMD are very low, their large-scale impacts confirm that the skin effects of the electromagnetic field cannot be neglected. The skin depth can be written as

$$d = \sqrt{1/\pi f \mu \gamma}, \tag{10}$$

where $\mu = \mu_0, f$ is 0.001–0.1 Hz [16], and the conductivity γ is 0.001–4 S/m. Equation (10) indicates that the skin depth depends on f and γ. The calculated results show that the skin depth can reach hundreds or even several thousand kilometers. Magnetotelluric data demonstrate that the conductivity of land is generally 0.1–0.00001 S/m, whereas the conductivity below 100 km generally exceeds 0.01 S/m [20]. Since the lower boundary is deeper than 500 km below ground, where the electromagnetic field attenuates to a small value compared to the field at the air-Earth interface, the lower boundary condition is set to

$$\boldsymbol{A} = 0. \tag{11}$$

III. SIMPLIFICATION OF MODEL AND METHODS

A. SIMPLIFIED BLOCK MODEL

We set the space current direction parallel to the interface between the two regions, and assume that both the space current and the Earth model has infinite extent in the y-direction, and that the source current and ground conductivity does not change along the y-direction. The eddy current field is parallel to the y-axis, and the magnetic vector potential has only a y-component. The magnetic field intensity has x- and z-components, and the electric field intensity and induced current have only y-components. Thus, the problem can be simplified to a 2-D field problem in the x–z plane. In electromagnetic calculations, the finite element method (FEM) can be employed to simulate 2-D or 3-D models by using the Galerkin method of weighted residuals [21]. Therefore, we adopt the FEM to model the lateral variations of the Earth conductivity structures [22].

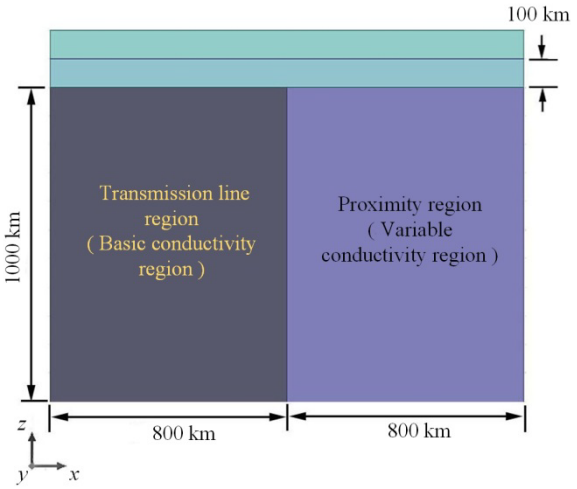

FIGURE 3. Simplified 2-D block model for E-field calculation.

The 2-D approximation of the proximity effect model is shown in Fig. 3. The origin is set at the conductive interface, with x pointing in the direction of the conductivity changes and z pointing upwards. The maximum depth of the model should exceed the skin depth. The transmission line is located in the basic conductivity region where $x < 0$, where the conductivity is set to 0.01 S/m, which is commonly seen in rocks containing slight amounts of water. The conductivity in the proximity region $x > 0$ is set to $0.01k$ S/m. The conductivity change coefficient k represents the Earth conductivity variations and is set between 1 and 100.

B. GOVERNING EQUATIONS AND BOUNDARY CONDITIONS

The 2-D eddy current field is a parallel plane field along the y-axis. The unknown variable, the magnetic vector potential, only has a y-component and satisfies the Coulomb gauge equation $\nabla \cdot \boldsymbol{A} = 0$; thus, it can be solved using the scalar A_y. The scalar potential satisfies $\nabla\varphi = \frac{\partial\varphi}{\partial y}\boldsymbol{e}_y = 0$. The governing equations can be written as

$$-\frac{1}{\mu}\nabla^2 A_y + j\omega\gamma A_y = J_{sy} \tag{12}$$

and

$$-\frac{1}{\mu}\left(\frac{\partial^2 A_y}{\partial x^2} + \frac{\partial^2 A_y}{\partial z^2}\right) + j\omega\gamma A_y = J_{sy}. \tag{13}$$

The surface current density J_{sy} is $\sin\omega t A/m$. Since the lower boundary is sufficiently far from the current source,

the y-component of the magnetic vector potential attenuates to zero: $A_y\big|_{z=-\infty} = 0$. According to the horizontal source current distribution, $-\frac{1}{\mu}\frac{\partial A_y}{\partial n}\Big|_{z=100} = J_{sy}$. We assume that the media near the left and right boundaries of solution region are uniform in the x-direction, so the magnetic field is perpendicular to the left and right boundaries, $H_t = -\frac{1}{\mu}\frac{\partial A_y}{\partial n}\Big|_{x=-800,800} = 0$, where t points in the tangential direction.

After A_y is determined, the magnetic flux intensity, electric field intensity, and telluric currents can all be determined readily using (14) and (15).

$$\boldsymbol{B} = \nabla \times \boldsymbol{A} = -\frac{\partial A_y}{\partial z}\boldsymbol{e}_x + \frac{\partial A_y}{\partial x}\boldsymbol{e}_z. \tag{14}$$

$$\boldsymbol{E} = -\frac{\partial A_y}{\partial t}\boldsymbol{e}_y. \tag{15}$$

C. PARAMETERS FOR ANALYSIS OF E-FIELD INTENSITY

In this study, we extract the amplitude of the surface electric field intensity to analyze the electric field amplitude distribution on the horizontal plane and employ the following parameters:

E_{y2}: the reference value of the electric field intensity in the variable conductivity region;

E_{y1}: the reference value of the electric field intensity in the basic conductivity region;

$\Delta E_{y2} = E_{y2}$-E_{y1}: the difference between the reference values of the geoelectric field, which is only related to k and f;

$E_y(x)$: the intensity of the component of the geoelectric field parallel to the boundary as a function of perpendicular distance x from the discontinuity in conductivity at the boundary between the two conductivity regions;

$\Delta E_y(x) = E_y(x)$-E_{y1}: the amplitude variation of the electric field intensity as a function of perpendicular distance from the discontinuity in the conductivity.

We suppose that the region in which the distance from the interface is less than x km would be influenced by abrupt lateral conductivity change when $\Delta E_y(x) > 0.1E_{y1}$. Thus, we define a 10% influence range $x_{10\%}$ using $\Delta E_y(x_{10\%}) = 0.1E_{y1}$. The ratio between the wave impedances on the two sides of the interface is

$$Z_c \Big/ Z_b = \sqrt{1/k}. \tag{16}$$

The ratio between the electric field intensities in the two regions can be expressed as

$$E_{yc} \Big/ E_{yb} = \sqrt{1/k}. \tag{17}$$

Therefore, when $1 < k < 1.21$, the influence of abrupt lateral conductivity change on the geoelectric field can be neglected.

IV. NUMERICAL RESULTS

A. ELECTRIC FIELD DISTRIBUTION

In this study, f is 0.001–0.1 Hz and k is 1–100. For $f = 0.001$ Hz and $k = 10$, the magnetic induction and electric field intensity distributions are presented in Figs. 4(a) and 4(b), respectively, as examples. The maximum amplitude of the magnetic flux density occurs at the interface and is about 1600 nT, which is on the order of magnitude of flux density change at auroral latitudes during a GMD. The rate of change of the magnetic flux density is 384 nT/min, which is on the order of the magnitude of the rate of change of GMD intensity at mid-low latitudes during an intense GMD. In this case, E_{y1} and E_{y2} are 0.887 V/km and 0.280 V/km, respectively, making $\Delta E_{y2} = E_{y2}$-$E_{y1} = 0.607$ V/km. This gives the proximity-to-base E-field ratio $E_{y2}/E_{y1} \approx \sqrt{1/10} = \sqrt{1/k}$, which agrees well with the wave impedance ratio. The results shown in Fig. 4(b) are consistent with the analytic solution provided by the plane wave method [23], namely that the intensity of the electric

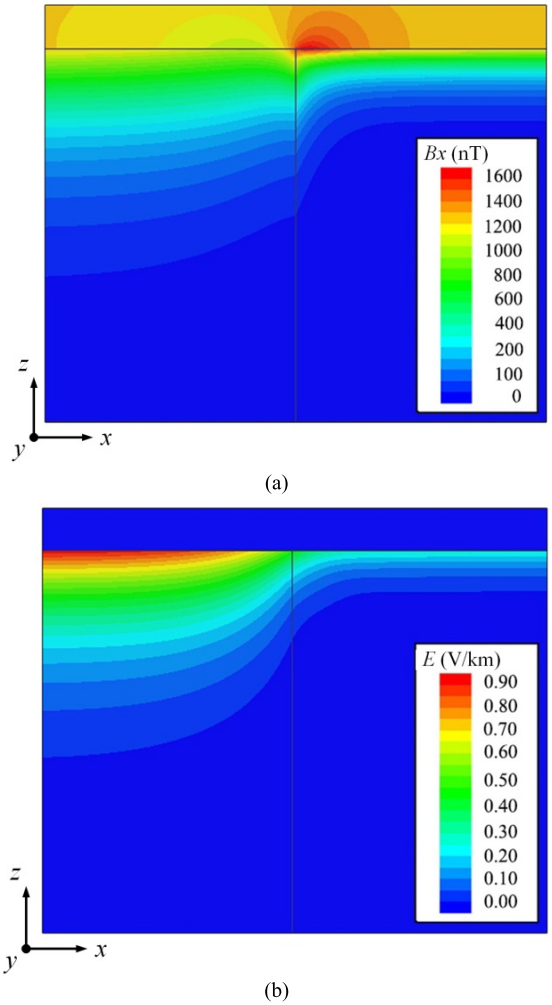

FIGURE 4. Field distributions from the surface of the Earth to a depth of 500 km obtained with $f = 0.001$ Hz and $k = 10$. (a) Magnetic field distribution (b) Electric field distribution.

field in a low-conductance region is higher than in an adjacent high-conductance region. And the consequences also demonstrate that proximity effect decreases the y-component of the electric field in a low-conductance area and increases it in a high-conductance area. The distance from the interface, space current frequency, and k all impact the electric field amplitude variations.

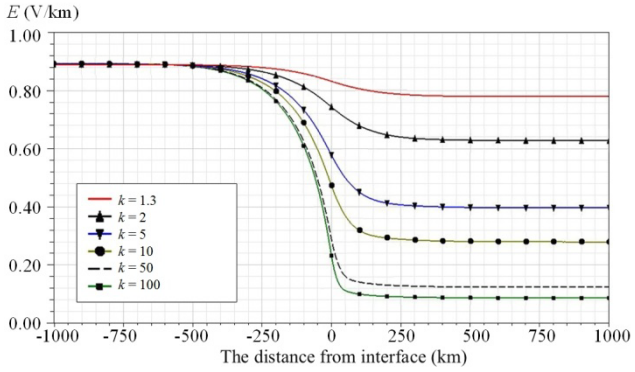

FIGURE 5. Geoelectric field distributions at the surface of the Earth within 1000 km from the discontinuity with $f = 0.001$ Hz and $k = 1.3$, 2, 5, 10, 50, and 100.

For the GIC calculations, we focus on the geoelectric field distribution near the surface of the Earth, which is shown in Fig. 5. The origin is set at the interface, with the x-axis extending from -800 km to 800 km. The results show that the greater the conductivity difference is, the more sharply the electric field decreases. The range over which the transition in the amplitude of the E-field occurs extends to about 250 km from the interface into the transmission line region.

In addition, the relationships between $x_{10\%}$ and f and k are investigated. For instance, with $k = 10$ and $f = 0.003$ Hz, we obtain $x_{10\%} = 160$ km and $\Delta E_y(50) = 0.393$ V/km, which is 24.9% of E_{y1} and 36.4% of ΔE_y. The results demonstrate that the proximity effect apparently has a significant influence on the electric field at a distance of 50 km from the discontinuity. Taking f as an independent variable and setting k equal to 2, 10, and 100 respectively, the values of $x_{10\%}$ presented in Fig. 6(a) are obtained. With increasing f, $x_{10\%}$ decreases gradually. Analogously, k is set as an independent variable and f is set equal to 0.01 Hz and 0.001Hz to obtain the $x_{10\%}$ values shown in Fig. 6(b). Therefore, the $x_{10\%}$ parameter decreases rapidly with increasing f, but it has only a weak dependence on k.

B. INFLUENCE OF PROXIMITY EFFECT ON GIC

A discontinuity in the conductivity of the Earth affects the magnitude of a geoelectric field which has a polarization that is parallel to the discontinuity. The magnitude changes with distance perpendicular to the conductivity change. If a transmission line is parallel to the conductivity interface, the GIC will be affected by discontinuity in the conductivity of the Earth. Therefore, we investigate the influence of a discontinuity in the conductivity on the electric field intensity

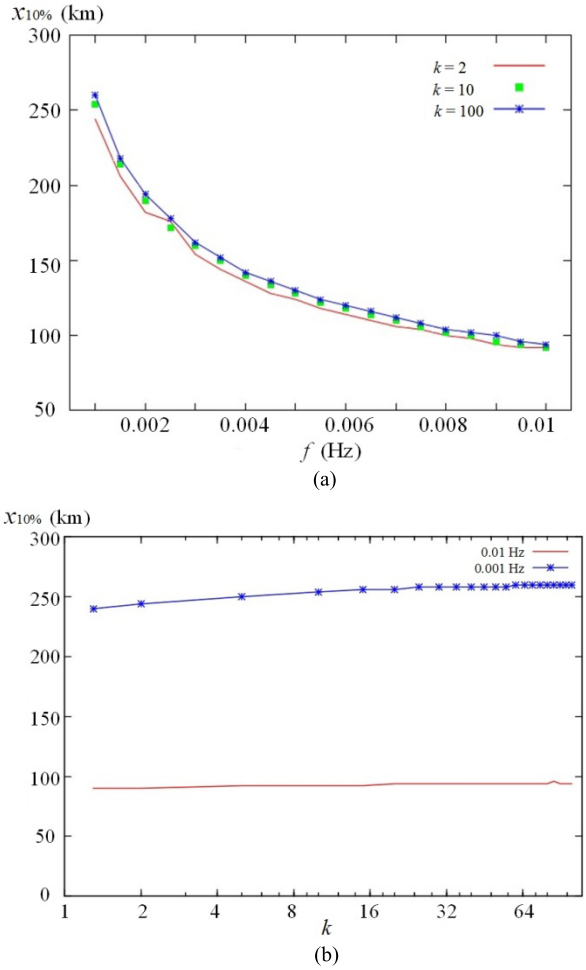

FIGURE 6. Relationship between $x_{10\%}$ and model parameters. (a) $x_{10\%}$ *vs.* f with k as parameter. b) $x_{10\%}$ *vs.* k with f as parameter.

at substations at various distances from the discontinuity. Taking k as an independent variable, the electric field intensities $E_y(10)$ and $E_y(50)$ shown in Figs. 7(a) and 7(b), respectively, are obtained. The influence of the discontinuity in the conductivity on the geoelectric field increases with proximity to the discontinuity. The parameter k affects ΔE_{y2}, and $E_y(10)$ is indirectly affected by the proximity to the discontinuity. Therefore, the electric field variation from the base value for a homogeneous Earth increases with increasing conductivity difference between the adjacent conductivity regions.

We also investigate the influences of the conductivity changes and the distance between the substation and the discontinuity in conductivity on the GIC in power grids. We assume that the transmission line is parallel to the discontinuity and do not account for GIC injection from other lines. Given the equivalent resistance of the transformer and transmission line, the GIC are calculated using

$$\mathrm{GIC} = \frac{|E| \cdot L}{R_L}, \tag{18}$$

where L is the effective length of the power transmission line between grounded power stations and R_L is the sum of the

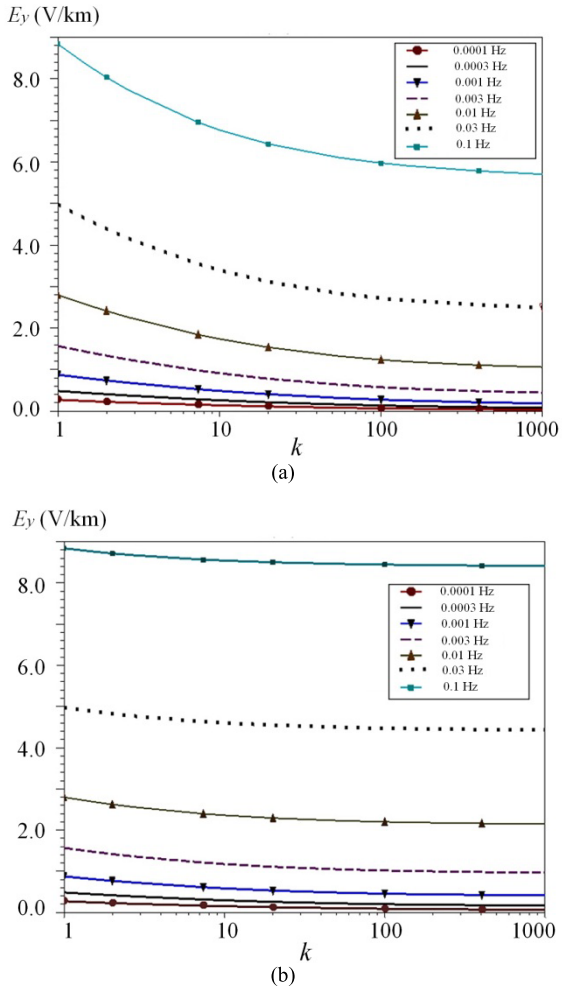

FIGURE 7. Variation of E_y with k. (a) E_y 10 km from the discontinuity in conductivity. (b) E_y 50 km from the discontinuity in conductivity.

equivalent DC resistances of the power line and substation. As an example, we consider a 50-km-long power line parallel to the discontinuity. The DC resistance is 2.5 Ω. The GIC caused by the E-field with polarization parallel to the discontinuity in conductivity are shown in Table 1. The results in the $k = 1$ case can be regarded as the GIC in the absence of a discontinuity in conductivity. The conductivity variations in the proximity region do not affect the electric field in the basic conductivity region far from the interface, and E_{y1} remains unchanged. Thus, by comparing the quantitative results derived from the $k = 1.5$, 2, 10, 100, and 1000 cases with those from the $k = 1$ case, we are able to determine the influence of the discontinuity in conductivity on the GIC.

TABLE 1. Amplitude of gic due to proximity of a discontinuity in earth conductivity, $f = 0.001$ Hz.

Distance (km)	$k = 1$	$k = 1.5$	$k = 2$	$k = 10$	$k = 100$	$k = 1000$
5	17.76	16.07	14.94	9.735	5.228	3.150
10	17.76	16.11	15.02	10.00	5.793	4.017
50	17.76	16.45	15.62	11.95	9.387	8.527

With the other parameters unchanged, the results show that the GIC decreases as k increases. When $k > 1$, the GIC are less than the reference value, which here refers to the value calculated for $k = 1$ using the plane wave method. Likewise, when $k < 1$, the GIC is greater than the reference value. Thus, the proximity effect becomes more serious for a line parallel to the discontinuity in conductivity as the distance between the discontinuity and the transmission line decreases and the line is parallel to the interface.

Since the electric field in the basic conductivity region is correlated with f, the ratios between the GIC with and without considering a lateral discontinuity in the conductivity at different frequencies are calculated to explore the effects of f on the GIC.

TABLE 2. Ratios Between GIC Values at different frequencies With and Without Considering proximity of a discontinuity in earth conductivity $k = 10$.

Distance (km)	0.0001 Hz	0.0003 Hz	0.001 Hz	0.003 Hz	0.01 Hz	0.03 Hz	0.1 Hz
5	0.529	0.541	0.548	0.560	0.579	0.612	0.667
10	0.534	0.550	0.563	0.586	0.623	0.682	0.766
50	0.576	0.618	0.673	0.751	0.844	0.925	0.966

The results, shown in Table 2, indicate that with the same parameters, the range of influence of the discontinuity in the conductivity decreases as f increases. For the same line, the discontinuity in the Earth's conductivity affects the low-frequency components of the GIC in the line more than the high-frequency components since for lower frequencies the range of influence of the conductivity in the proximity region extends further into the transmission line region.

V. CONCLUSION

In this paper, a block model for analyzing the proximity effect is established. The FEM is used to solve the boundary value problem of eddy current fields. We then obtain the geoelectric field distribution in the presence of a parallel discontinuity in the Earth conductivity. Based on the parameters of typical lines, a two-node model is analyzed to investigate the influence of the lateral variations of the Earth conductivity on the GIC in a power line parallel to the discontinuity in the conductivity. The results indicate that lateral variations in the Earth conductivity in a region proximal to the power line can affect the GIC in the power line. The main results are as follows.

1) The proximity effect influences the magnitude of a geoelectric field vector which is parallel to a lateral discontinuity in the conductivity of the Earth. The magnitude of the E-field varies with distance perpendicular to the discontinuity in the Earth. The E-field increases as the distance to the discontinuity decreases when there is a proximal low conductance areas and decreases with decreasing distance to the discontinuity when there is a proximal high-conductance area so that the

tangential component of the geoelectric field at the interface between the areas with different conductivities remains continuous. The greater the difference between the conductivities on the two sides of the discontinuity, the greater the difference between the surface electric fields on the two sides, and the more significant the influence of the proximity effect.

2) For a typical f, the geoelectric field distortion does not exceed 10% of the reference value in the region more than 250 km from the interface. Thus, the influence of the proximity effect is only observable within 250 km. This range is related to f but is only weakly dependent on k.

3) The proximity of a discontinuity in conductivity of the Earth affects the GIC in transmission lines that are running parallel to the discontinuity. The GIC affected by the proximity effect will be greater than the reference value (the GIC without considering the proximity effect) when the adjacent area has low conductivity, and it will be lower than the baseline value when the adjacent area has high conductivity. For typical geological structures and geomagnetic storms, the influence range of a discontinuity in conductivity on the GIC is 80–250 km. For example, if there is a region with low conductivity within a perpendicular distance of 50 km from the discontinuity in the conductivity, the proximity effect increases the GIC by 10%–30%. Therefore, to assess GIC in complex geological structures, we should consider the Earth conductivity not only in the area in which the line is located, but also in the area adjacent to that containing the line.

In the case of an E-field with polarization perpendicular to a discontinuity in Earth conductivity, which is described by Gilbert [24] as the ''H-polarization'' case, the discontinuity causes the magnitude of the geoelectric field to increase sharply with proximity to the discontinuity between a region of low conductivity and a region of high conductivity such as at the ocean-land interface [13]. In a subsequent work, we will discuss in detail the effects on the geoelectric fields and GIC induced during magnetic storms of a discontinuity in Earth conductivity for the H-polarization case.

REFERENCES

[1] C.-M. Liu, L.-G. Liu, and R. Pirjola, ''Geomagnetically induced currents in the high-voltage power grid in China,'' *IEEE Trans. Power Del.*, vol. 24, no. 4, pp. 2368–2374, Oct. 2009.

[2] J. G. Kappernman and V. D. Albertson, ''Bracing for the geomagnetic storms,'' *IEEE Spectr.*, vol. 27, no. 3, pp. 27–33, Mar. 1990.

[3] R. Pirjola, D. Boteler, A. Viljanen, and O. Amm, ''Prediction of geomagnetically induced currents in power transmission systems,'' *Adv. Space Res.*, vol. 26, no. 1, pp. 5–14, 2000.

[4] B. Dong, D. W. Danskin, R. J. Pirjola, D. H. Boteler, and Z. Z. Wang, ''Evaluating the applicability of the finite element method for modelling of geoelectric fields,'' *Ann. Geophys.*, vol. 31, no. 10, pp. 1689–1698, 2013.

[5] R. Pirjola, ''Geomagnetically induced currents during magnetic storms,'' *IEEE Trans. Plasma Sci.*, vol. 28, no. 6, pp. 1867–1873, Dec. 2000.

[6] J. F. Hermance and W. R. Peltier, ''Magnetotelluric fields of a line current,'' *J. Geophys. Res.*, vol. 75, no. 17, pp. 3351–3356, Jun. 1970.

[7] J. T. Weaver, ''The electromagnetic field within a discontinuous conductor with reference to geomagnetic micropulsations near a coastline,'' *Can. J. Phys.*, vol. 41, no. 3, pp. 484–495, 1963.

[8] F. W. Jones and A. T. Price, ''The perturbations of alternating geomagnetic fields by conductivity anomalies,'' *Geophys. J. Int.*, vol. 20, no. 3, pp. 317–334, Aug. 1970.

[9] F. W. Jones and A. T. Price, ''The geomagnetic effects of two-dimensional conductivity inhomogeneities at different depths,'' *Geophys. J. Int.*, vol. 22, no. 4, pp. 333–345, Apr. 1971.

[10] W. D. Parkinson and F. W. Jones, ''The geomagnetic coast effect,'' *Rev. Geophys.*, vol. 17, no. 8, pp. 1999–2015, 1979.

[11] C. Liu, Y. Li, and R. Pirjola, ''Observations and modeling of GIC in the Chinese large-scale high-voltage power networks,'' *J. Space Weather Space Clim.*, vol. 4, p. A03, Jan. 2014.

[12] D. Bo, W. Ze-Zhong, L. I. U. Lian-Guang, L. I. U. Li-Ping, and L. I. U. Chun-Ming ''Proximity effect on the induced geoelectric field at the lateral interface of different conductivity structures during geomagnetic storms,'' (in Chinese), *Chin. J. Geophys.*, vol. 58, no. 1, pp. 32–40, 2015.

[13] R. Pirjola, ''Practical model applicable to investigating the coast effect on the geoelectric field in connection with studies of geomagnetically induced currents,'' *Adv. Appl. Phys.*, vol. 1, no. 1, pp. 9–28, 2013.

[14] W. Zezhong, D. Bo, and L. Chunming, ''Earth conductivity modelling technique for calculation geoelectric field during geomagnetic storms,'' *Sci. Technol. Eng.*, vol. 15, no. 13, pp. 72–76, 2015.

[15] J. G. Kappenman, ''Storm sudden commencement events and the associated geomagnetically induced current risks to ground-based systems at low-latitude and midlatitude locations,'' *Space Weather*, vol. 1, no. 3, p. 1016, 2003.

[16] V. D. Albertson and J. A. Van Baelen, ''Electric and magnetic fields at the Earth's surface due to auroral currents,'' *IEEE Trans. Power App. Syst.*, vol. PAS-89, no. 4, pp. 578–584, Apr. 1970.

[17] K. Zheng, R. J. Pirjola, D. H. Boteler, and L. G. Liu, ''Geoelectric fields due to small-scale and large-scale source currents,'' *IEEE Trans. Power Del.*, vol. 28, no. 1, pp. 442–449, Jan. 2013.

[18] B. Dong, Z. Wang, R. Pirjola, C. Liu, and L. Liu, ''An approach to model Earth conductivity structures with lateral changes for calculating induced currents and geoelectric fields during geomagnetic disturbances,'' *Math. Problems Eng.*, vol. 2015, no. 2, 2015, Art. no. 761964.

[19] V. D. Albertson, J. M. Thorson, Jr., and S. A. Miske, Jr., ''The effects of geomagnetic storms on electrical power systems,'' *IEEE Trans. Power App. Syst.*, vol. PAS-93, no. 4, pp. 1031–1044, Jul. 1974.

[20] Y. J. Shi, G. D. Liu, and G. Y. Wu, *Magnetotelluric Sounding Tutorial*. Beijing, China: Seismological Press, 1985.

[21] D. S. Pipkins and S. N. Atluri, ''Applications of the three dimensional finite element alternating method,'' *Finite Elem. Anal. Des.*, vol. 23, pp. 133–153, Nov. 1996.

[22] E. Matandirotya, P. J. Cilliers, and R. R. Van Zyl, ''Modeling geomagnetically induced currents in the South African power transmission network using the finite element method,'' *Space Weather*, vol. 13, no. 3, pp. 185–195, 2015.

[23] L. Cagniard, ''Basic theory of the magneto-telluric method of geophysical prospecting,'' *Geophysics*, vol. 18, no. 3, pp. 605–635, 1953.

[24] J. L. Gilbert, ''Modeling the effect of the ocean-land interface on induced electric fields during geomagnetic storms,'' *Space Weather*, vol. 3, no. 4, pp. 1–9, 2005.

CHUNMING LIU was born in Hebei, China, in 1972. He received the B.S. degree in mechanical engineering from the Hebei University of Technology, China, in 1993, and the M.S. and Ph.D. degrees in electrical engineering from North China Electric Power University, in 2000 and 2009, respectively.

He has been a Professor with North China Electric Power University. His current research interests include geomagnetically induced currents in power grids, including monitoring, modeling, and assessing the influence on the security of power systems.

XUAN WANG received the B.S. degree from the Hebei University of Technology, China, in 2014. She is currently pursuing the Ph.D. degree with the School of Electrical and Electronic Engineering, North China Electric Power University, Beijing, China.

Her research interests include risk assessment of magnetic storm and prevention and control of power grid disaster.

CHENXIANG LIN received the B.S. and M.S. degrees in electrical engineering from North China Electric Power University, China.

He is currently an Electrical Engineer with the Electric Power Research Institute, State Grid of Fujian, China. His research interests include geomagnetically induced current in power grids and HVDC flexible and relay protection systems.

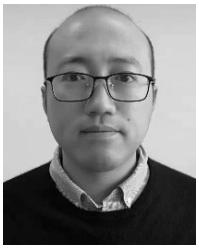

JINGYU SONG received the M.S. degree from Xi'an Jiaotong University, China.

He is currently an R&D Engineer with the China State Shipbuilding Corporation System Engineering Research Institute. His research interests include system engineering and electrical engineering.